A referenced beatnote interrogated biosensor based on coupled DBR laser cavities

W.A.P.M. Hendriks, Sonia M. Garcia-Blanco

MESA+ Institute, University of Twente, P.O. Box 217, 7550 AE, Enschede, The Netherlands

Resonance sensors have been shown to be highly sensitive [1], [2]. Their performance is, however, limited by the presence of noise in the signal amplitude and in the resonance position of the resonator [3]. In addition, the need for low linewidth very stable tunable lasers increases cost and limits on chip integration[4]. To overcome both the noise and integration limitations we propose a biosensor based on two coupled DBR laser cavities. We will discuss the expected sensitivity and the effect of temperature stability. Finally, we will show the expected limit of detection for the sensor.

Introduction

Due to their versatility and high sensitivity, optical resonance sensors are of interest for many applications[1], [2], [5], [6]. The resonances shifts are usually tracked by scanning a tunable laser over the resonance repeatedly or using a spectrometer with a broad band source to acquire the resonance position. While both configurations can be implemented on chip for a single use sensor the requirements on the tunable source or spectrometer to obtain high quality sensors are stringent[3], [7]. Especially the need for high spectral resolution and spectral stability over long time periods complicate the implementation on chip. The spectral stability is especially limited by thermal crosstalk when the source sensor and detector are integrated on one chip[8]. In order to circumvent the need for tunable lasers or spectrometers we present a novel sensor configuration based on two coupled Distributed Bragg reflector cavities, as schematically presented in Figure 1 (A).

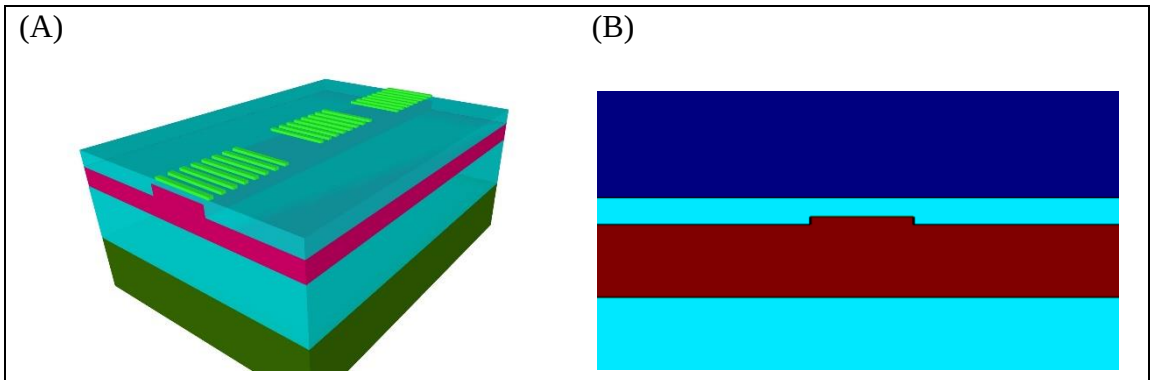

Figure 1. (A) Schematic representation of the coupled DBR cavity biosensor for referenced beatnote detection. The red area indicates the aluminium oxide waveguide layer. The silicon dioxide substrate and upper cladding layers are indicated in blue. The grating material or etch positions are indicated in light green.(B) Cross section of the waveguide geometry, where the light blue layer indicates the SiO_2 substrate and cladding layer and red indicates the Al_2O_3 core and finally the dark blue indicates the analyte which we assume to be water.

The sensor consists of two DBR laser cavities each consisting of an ytterbium doped Al_2O_3 ridge waveguide on both ends terminated by a Bragg reflector. DBR lasers in this material have been shown to exhibit high efficiency and low thresholds[9]. For the proposed sensor the fields of the individual cavities are coupled by the transmission through the center grating, this coupling induces a splitting of the cavity modes[10].The

mode splitting allows for a heterodyne detection scheme as the split resonance induces a beatnote, where the beatnote frequency is given by the amount of resonance splitting. The grating strength and thus the beatnote frequency can be modulated by biomarker binding in the minima of the grating, as a result the transmission decreases resulting in a beatnote shift. Giving a response that is sensitive to biomarker binding while being in principle insensitive to small perturbations of the individual DBR cavities. For the sensor to exhibit the desired behavior a single longitudinal mode DBR laser is required, as shown by Bernhardi et.al.[9], [11]. The sensor will therefore be based on two of the described cavities coupled by an adjusted center grating mirror which will be the only altered component. The DBR cavities have a length of 2.5 mm with outcoupling mirrors with a length of 3.75 mm and a coupling coefficient of 6 cm^{-1}. The waveguide cross section consists of a 1 μm thick ytterbium doped Al_2O_3 layer into which a 90 nm high ridge waveguide is etched with a width of 2.5 μm as depicted in Figure 1 (B). The free design parameters for our sensor then become the strength and length of the coupling grating. In order to determine the optimal length and strength the system is modeled using a temporal coupled mode theory formalism[10].

Coupled cavity model

The temporal coupled mode theory description of a coupled cavity system is modeled gives the following set of coupled differential equations for the coupled cavity modes

$$\frac{d}{dt}\begin{bmatrix}a_1\\a_2\end{bmatrix}=\begin{bmatrix}j\omega_1 & \kappa_{12}\\ \kappa_{21} & j\omega_2\end{bmatrix}\begin{bmatrix}a_1\\a_2\end{bmatrix}, \tag{1}$$

where $a_{1,2}$ are the mode amplitudes of the respective cavities, with $\omega_{1,2}$ being the individual cavity resonances and κ_{12} and κ_{21} are the coupling from cavity 1 to cavity 2 and vice versa. Energy conservation imposes a restriction on κ, giving the relation $\kappa_{12} = -\kappa_{21}^{*}$. Assuming a time dependence of the form $e^{j\omega t}$ the eigenvalues of the system are given by,

$$\omega = \frac{\omega_1+\omega_2}{2} \pm \sqrt{\left(\frac{\omega_1-\omega_2}{2}\right)+|\kappa_{12}|^2}. \tag{2}$$

If we assume the resonance frequencies of the individual cavities are indistinguishable, we find the resonance splitting to be

$$\omega_{\text{beatnote}} = \Delta\omega = 2|\kappa_{12}|. \tag{3}$$

This coupling is defined as the energy that is transferred between the modes per unit time, this is related to the grating transmission by,

$$|\kappa_{12}| = t\frac{v_g}{2l_{eff}}, \tag{4}$$

where t is the grating transmission coefficient, $v_g$is the group velocity and l_{eff} is the effective cavity length which is the cavity length plus the penetration length (l_{pen}) into the Bragg reflectors of the cavity, given by,

$$L_{pen} = \frac{\tanh(\kappa_g l_g)}{2\kappa_g}, \tag{5}$$

where κ_g is the grating coupling coefficient and l_g is the length of the grating[12]. The maximum transmission coefficient of a Bragg grating is given by

$$t = \operatorname{sech}(\kappa_g l_g). \tag{6}$$

Finally, the grating coupling strength is given by,

$$\kappa_g = \frac{k}{2\pi n_{eff}}\left(n_{clad}^2 - n_{analyte}^2\right)\sin(\pi D)\,\Gamma_{grating}, \tag{7}$$

where k is the free space wave vector, $n_{eff}, n_{clad}, n_{analyte}$ are the refractive indices of the unperturbed waveguide mode, the waveguide cladding and, D is the duty cycle of the grating and $\Gamma_{grating}$ is the field overlap with the grating region of the waveguide cross section[13]. Combining equation 3 to 7 we find an expression for the beatnote frequency,

$$\omega_{beatnote} = \operatorname{sech}\left(\frac{k}{2\pi n_{eff}}\left(n_{clad}^2 - n_{analyte}^2\right)\sin(\pi D)\,\Gamma_{grating} l_g\right)\frac{v_g}{2l_{eff}}. \tag{8}$$

Sensitivity

As is obvious from equation 8 the change in beatnote will be maximal when the field overlap with the analyte is maximal, therefore the coupling grating in the 340 nm thick SiO_2 cladding will be etched fully until the Al_2O_3.In addition the sensitivity will be maximal when the duty cycle is 50% as this is the maximum of the sine. The remaining parameters for equation 8 are then calculated using Lumerical Mode[14], where we assume a refractive index for the SiO_2 of 1.45 and 1.67 for Al2O3, to find an effective refractive index for the fundamental TE mode of 1.63 , a group velocity of $1.723 \cdot 10^8 m/s$ and a field overlap with the grating region of 2.6%. The resulting dependence of the beatnote for the found parameters on the grating length is shown Figure 2 (A). To obtain the optimal grating length we find the minimal slope of the response at 0.16 mm. For the found optimal coupling grating length the refractive index in the low index period of the grating is varied between 1.33 and 1.34 to obtain a refractive index sensitivity of 87Ghz/RIU.

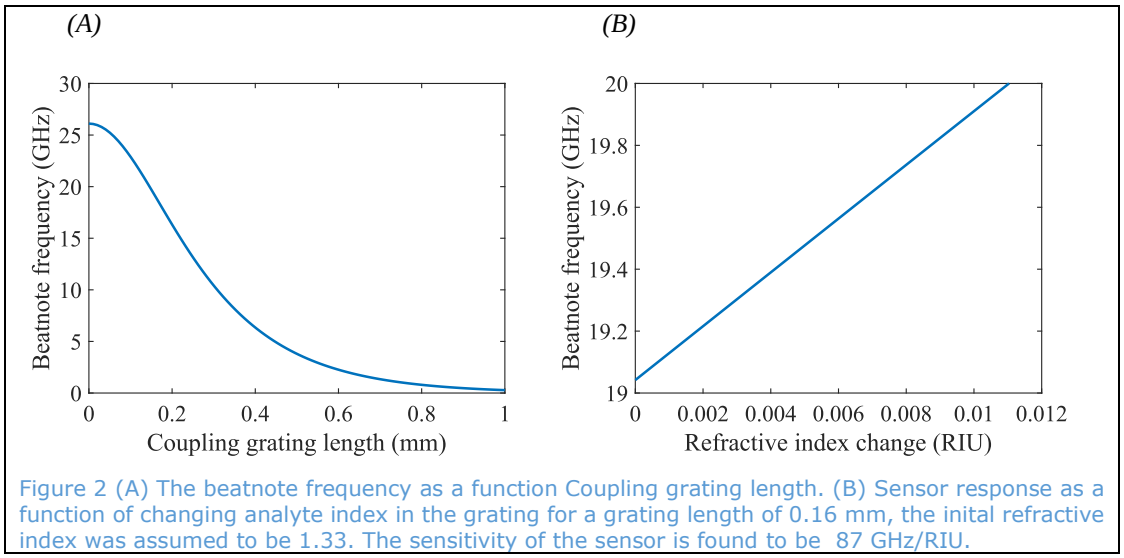

Figure 2 (A) The beatnote frequency as a function Coupling grating length. (B) Sensor response as a function of changing analyte index in the grating for a grating length of 0.16 mm, the inital refractive index was assumed to be 1.33. The sensitivity of the sensor is found to be 87 GHz/RIU.

Limit of Detection

The limit of detection of a sensor is defined as

$$LOD = \frac{3\sigma}{S}, \tag{9}$$

where σ is the variance of the sensor response. The variance of the beatnote response for our design will most likely be dominated by the inevitable changing difference in the natural frequencies of the cavities, which can be expressed as,

$$\Delta\omega_i = \frac{\Delta_{env} n_{eff} \omega_{res}}{n_g}, \tag{10}$$

Where $\Delta_{env} n_{eff}$ is the effective index shift caused by an environmental change, which can be expressed as, $\Delta_{env} n_{eff} = c\int \Delta\varepsilon(x,y)\boldsymbol{E}_s \cdot \boldsymbol{E}_s^* \, dxdy$ [10], [15]. Assuming the waveguide cross section is identical over the entire length of both cavities, the change in the resonance frequency would completely cancel, this is however not likely. We will therefore analyze the resonance shift as a function of temperature variations as temperature is likely to dominate the noise of the sensor. Assuming a temperature variance of 1mK we find for a temperature coefficient of $1.86 \cdot 10^{-5} K^{-1}$ for Al_2O_3[16] a variance of 10Mhz. Resulting in a upper limit for the limit of detection in the order of $10^{-4} RIU$

Conclusion

Based on existing DBR laser cavity implementations, a novel sensor design is presented with a sensitivity of 87GHz/RIU. With an expected limit of detection below $10^{-4} RIU$. Furthermore, the simplicity of the total package of the sensor opens up opportunities for the development of one-time use implementations.

References

[1] M. de Goede *et al.*, "Al_2O_3 microring resonators for the detection of a cancer biomarker in undiluted urine," *Opt. Express*, vol. 27, no. 13, p. 18508, Jun. 2019.

[2] M. Iqbal *et al.*, "Label-free biosensor arrays based on silicon ring resonators and high-speed optical scanning instrumentation," *IEEE J. Sel. Top. Quantum Electron.*, vol. 16, no. 3, pp. 654–661, 2010.

[3] I. M. White and X. Fan, "On the performance quantification of resonant refractive index sensors," *Opt. Express*, vol. 16, no. 2, p. 1020, Jan. 2008.

[4] Y. Sun and X. Fan, "Optical ring resonators for biochemical and chemical sensing," *Anal. Bioanal. Chem.*, vol. 399, no. 1, pp. 205–211, 2011.

[5] X. Fan, I. M. White, S. I. Shopova, H. Zhu, J. D. Suter, and Y. Sun, "Sensitive optical biosensors for unlabeled targets: A review," *Anal. Chim. Acta*, vol. 620, no. 1–2, pp. 8–26, Jul. 2008.

[6] R. I. Stoian, B. K. Lavine, and A. T. Rosenberger, "pH sensing using whispering gallery modes of a silica hollow bottle resonator," *Talanta*, vol. 194, pp. 585–590, 2019.

[7] A. V. Velasco *et al.*, "High-resolution Fourier-transform spectrometer chip with microphotonic silicon spiral waveguides," *Opt. Lett.*, vol. 38, no. 5, p. 706, Mar. 2013.

[8] Y. Fan, "Semiconductor-glass waveguide hybrid lasers with ultra-high spectral purity," PhD thesis, University of Twente, 2017.

[9] E. H. Bernhardi, H. A. G. M. van Wolferen, K. Wörhoff, R. M. de Ridder, and M. Pollnau, "Highly efficient, low-threshold monolithic distributed-Bragg-reflector channel waveguide laser in Al_2O_3:Yb^{3+}," *Opt. Lett.*, vol. 36, no. 5, p. 603, Mar. 2011.

[10] H. A. Haus, *Waves and fields in optoelectronics TT* -. Englewood Cliffs, NJ : Prentice-Hall,.

[11] E. H. Bernhardi, *Bragg-grating-based rare-earth-ion-doped channel waveguide lasers and their applications*. 2012.

[12] D. I. Babic and S. W. Corzine, "Analytic expressions for the reflection delay, penetration depth, and absorptance of quarter-wave dielectric mirrors," *IEEE J. Quantum Electron.*, vol. 28, no. 2, pp. 514–524, 1992.

[13] T. E. Murphy, "Design, Fabrication and Measurement of Integrated Bragg Grating Optical Filters," 1994.

[14] I. Lumerical Solutions, "Lumerical.", www.lumerical.com.

[15] W. Bogaerts *et al.*, "Silicon microring resonators," *Laser Photon. Rev.*, vol. 6, no. 1, pp. 47–73, Jan. 2012.

[16] C. C. Kores, N. Ismail, D. Geskus, M. Dijkstra, E. H. Bernhardi, and M. Pollnau, "Temperature dependence of the spectral characteristics of distributed-feedback resonators," *Opt. Express*, vol. 26, no. 4, p. 4892, Feb. 2018.